Weathering trajectory of bauxite residue mud as predicted by high-temperature treatment

Talitha C Santini[a,*], Martin V Fey[a], Robert J Gilkes[a]

[a] School of Earth and Environment, University of Western Australia, M087, 35 Stirling Highway, Crawley WA 6009.
[*] email: santit01@student.uwa.edu.au

Abstract
Weathering of parent materials, an essential part of soil formation, can be a slow process in the field being partially constrained by reaction kinetics. Increasing temperature and pressure can accelerate attainment of chemical equilibrium. This study used pressure vessels to elevate temperature and pressure in order to rapidly determine the likely weathering trajectory of bauxite residue mud. Supernatant pH, EC, and alkalinity decreased over time with pH decreasing by 2.5 units after two days' treatment at 235°C. This behaviour suggests that residue mud has the capacity to 'auto-attenuate' porewater alkalinity and salinity without applied treatments. In the treated mud, gibbsite and tricalcium aluminate concentrations decreased whereas boehmite, hematite, goethite, calcite, sodalite, and muscovite increased in concentration relative to anatase. Precipitated hematite was more aluminous than the original hematite present in residue mud. Besides implications for the potential recovery of additional alumina from bauxite residue, the results suggest that residue alkalinity could be 'auto-attenuated' over very long (geological) periods of time.

Key Words
Bauxite residue, environmental remediation, weathering, reaction kinetics, alkalinity, salinity.

Introduction
Bauxite residue is an alkaline, saline, sodic slurry discharged to deposit areas as a by-product of the Bayer process. Bauxite residue mud (BRM) refers to the solid fraction of the slurry consisting of particles <150 μm in diameter (minimum 50% w/w of total solids). Despite dewatering and rinsing of the slurry, BRM is approximately 48% w/w solids suspended in pH 13 liquor. Leachate from BRM deposits continues to be collected through purpose built drainage systems after closure of deposit areas and it can maintain a pH > 10.5 for 20 years or more. Residue mud presents a greater long-term management challenge than residue sand (particles >150 in diameter) as (a) it is produced in greater quantities than residue sand; (b) it drains more slowly than sand, (c) entrained liquor maintains a higher pH despite extended rainwater leaching due to resupply of alkalinity by dissolution of minerals associated with this particle size fraction, and (d) its fine (and usually waterlogged) pores limit the rate of atmospheric carbonation.

Practices for rehabilitation of BRM deposits should be designed to accelerate natural mechanisms of alkalinity and salinity attenuation such as precipitation, dissolution, and leaching. The weathering trajectory of BRM therefore needs to be identified. Weathering of parent materials, an essential part of soil formation, can be a slow process in the field, partially constrained by reaction kinetics. Increasing temperature and pressure can accelerate attainment of chemical equilibrium. This study used pressure vessels to elevate temperature and pressure in order to rapidly determine the likely weathering trajectory of BRM.

Methods
Uncarbonated BRM was supplied by Alcoa World Alumina Australia (Kwinana refinery, Western Australia). Five temperatures (100, 130, 165, 200, and 235°C) were employed in order to generate kinetic data and identify reaction products. Each Teflon lined pressure vessel contained 4 g of residue (60% solids content) and 5 mL of MilliQ water, which was then heated to temperature in a rotating oven for up to 900 hours. Treated slurries were separated into liquid and solid phases by centrifugation. Supernatants were immediately filtered (0.2 μm cellulose acetate, Advantec MFS) and analysed for pH, EC, and total alkalinity by titration. Subsamples were acidified and stored at 4°C prior to ICP-OES analysis (PerkinElmer Optima 5300DV) for Al, Ca, Fe, K, Na, Si, and Ti. Treated solids were shaken with acetone to remove entrained solution, centrifuged and then airdried. Dried solids from 100, 165 and 235°C treatments were ground in an agate mortar and pestle and packed into glass capillaries for XRD analysis at the Powder Diffraction beamline (10BM1) at the Australian Synchrotron.

Peak locations and areas of selected minerals were calculated from synchrotron XRD patterns using Traces (v6.7.20, GBC Scientific Equipment Pty. Ltd. 2006). Naturally occurring anatase in the BRM was used as an internal standard for the purpose of comparing peak areas between patterns. Aluminium substitution was estimated for goethite using the d-spacings of the (110) and (111) reflections and the equation of Schulze (1984) and for hematite, using the *a* dimension as determined by least-squares refinement of (012), (104), (110), (113), (024), (116), (214), and (300) spacings and the equation of Schwertmann *et al*. (1979). Kinetic data were extracted from mineral peak areas observed in synchrotron XRD patterns using an approach identical to that of Murray *et al*. (2009). Mineralogical composition data was sourced from Taylor and Pearson (2001) and solution chemistry was determined by analysis of supernatants detailed above.

Results

Supernatant chemistry

pH, EC, and alkalinity all decreased at 165, 200, and 235°C (Figure 3). This indicates that BRM has the capacity to 'auto-attenuate'; that is, to lower its porewater alkalinity and salinity. Electrical conductivity and alkalinity increased over time for the 100 and 130°C treatments; however, the 165, 200, and 235°C treatments showed an initial increase relative to values for the unheated control, followed by a decrease over time in EC and alkalinity. These results suggest that the reaction is initially dominated by dissolution of the solid phase in contact with added water, and thereafter reflects chemical reactions that consume soluble alkalinity.

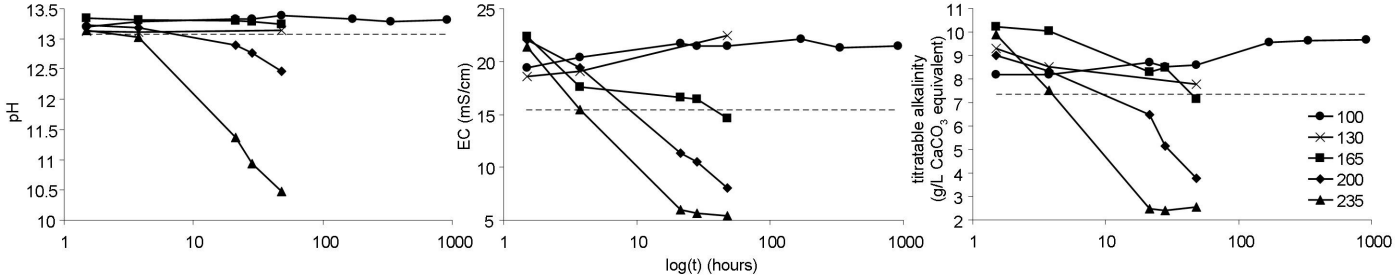

Figure 4. pH, EC and total alkalinity of supernatants from treated BRM. Dashed line indicates control values.

Solids mineralogy

Precipitation of iron and aluminium oxides, calcite, sodalite and muscovite are likely to be major mechanisms for lowering alkalinity and salinity in porewater, given the increase in XRD peak areas of these minerals compared to that of anatase (Table 1). Gibbsite dissolved and is likely to have been precipitated as boehmite. Tricalcium aluminate (TCA) dissolved more slowly than gibbsite and the Al and Ca supplied to solution are likely to have precipitated as boehmite and calcite, respectively. The hematite and goethite that precipitated during treatment appeared more aluminous than the original minerals in BRM, but remained within the ranges observed in other bauxite residue muds (4-12 mol% Al substitution in hematite and 17-35% mol% Al substitution in goethite) (Snars and Gilkes 2009).

Solution chemistry

ICP-OES analysis of supernatants after treatment showed net removal of Al, K, Na, and S from solution at temperatures ≥165°C (Figure 5). This agrees with observations of boehmite, sodalite, and muscovite precipitation. Iron concentrations in solution remained near or below the detection limit at all treatment temperatures except 235°C. Crystalline goethite and hematite may have formed from amorphous/nanocrystalline Fe oxides, which would account for little change of Fe in solution. Precipitation of Al-substituted Fe oxides also accounts for some removal of Al from solution. The assumption of anatase insolubility was supported by ICP-OES data, which indicated little Ti was released to solution except at 235°C. Titanium and iron were released simultaneously, which could indicate dissolution of a minor Fe-Ti phase. Ilmenite dissolution does not appear to account for this behaviour.

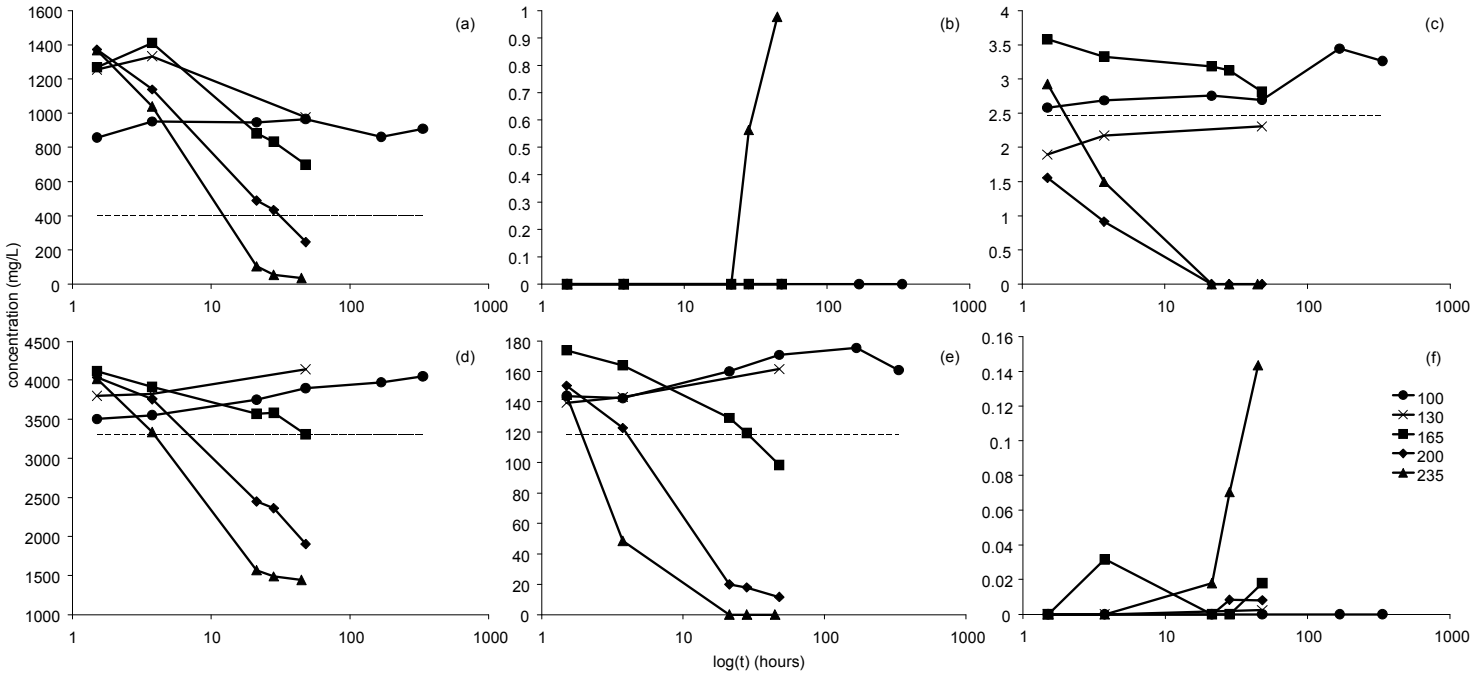

Figure 5. Concentrations of selected elements in treated supernatants, as determined by ICP-OES: (a) Al; (b) Fe; (c) K; (d) Na; (e) S; (f) Ti. Dashed lines indicate concentrations in control treatments. Where no dashed line is visible, concentrations in the control were below detection limits.

Table 1. Percentage change in mineral:anatase XRD reflection intensity ratio relative to untreated material. The ratio was calculated from primary peak areas of each mineral from synchrotron XRD patterns.

Temp (°C)	Time (hours)	Boehmite	Calcite	Gibbsite	Goethite	Hematite	Muscovite	Sodalite	TCA
100	1.5	82	30	54	47	15	16	47	41
100	21	102	43	47	48	29	25	62	24
100	48	153	44	46	52	30	44	64	-2
100	336	313	88	43	107	89	49	106	-2
165	1.5	300	53	-100	71	55	28	68	-14
165	21	468	95	-100	119	109	81	118	-100
165	48	584	106	-100	138	117	193	190	-100
235	1.5	348	85	-100	99	90	72	123	-35
235	3.8	526	88	-100	114	119	83	150	-100
235	21	587	94	-100	141	177	131	294	-100
235	48	643	111	-100	156	198	195	389	-100

Reaction kinetics

Sharp-Hancock analysis indicated that the plots of ln(-ln(1-a)) against ln(t) were well described by linear functions as r^2 values were generally >0.80, indicating that a single reaction mechanism likely dominated over the course of the reaction. This reaction mechanism may have been first-order surface controlled, because activation energies determined from Arrhenius plots ranged from 76 – 131 kJ/mol (Table 2), which is consistent with first-order surface controlled reaction kinetics. Reaction half-lives as predicted by the Avrami-Erofe'ev equation were predicted far more accurately by the first-order surface control model than for other models, for example three-dimensional (3D) diffusion control (Table 2). From the kinetic data presented in Table 2, it is possible to calculate the time required for reactions to proceed to a designated value of α at a designated temperature. This allows for extrapolation to field conditions, at an approximate temperature of 298K. Calcite, boehmite, goethite and hematite will reach half-completion within two centuries; however, muscovite and sodalite would take substantially longer to reach half-completion. This indicates that although 'auto-attenuation' of residues is possible, it will take millions of years to achieve chemical equilibrium in the field.

Table 2. Activation energies (E_a), frequency factors (A), and reaction rates (k) calculated from Arrhenius plots; reaction half-completion times ($t_{1/2}$) as calculated by interpolation of Sharp-Hancock lines of best fit to observed data (OB) and the Avrami-Erofe'ev equation predicted for first order surface control (FO) and 3D diffusion control (3D) (Francis *et al.* 1999) for mineral transformations in BRM.

		Calcite	Boehmite	Goethite	Hematite	Muscovite	Sodalite
Ea (kJ/mol)		100	88	76	76	94	131
ln A		18	13	10	8	13	21
$t_{(1/2)}$ at 508K (hours)	OB	0.00068	0.75	0.47	2.1	5.8	5.8
	FO	0.030	0.60	0.63	2.7	3.2	4.2
	3D	1.2	197	215	2738	3709	5879
$t_{(1/2)}$ at 298K (years)	FO	61	164	21	94	2396	1513193
log(k) (s^{-1})	508K	-2.2	-3.5	-3.5	-4.2	-4.2	-4.3
log(k) (s^{-1})	298K	-9.4	-9.9	-9.0	-9.6	-11	-14

Note: The rapid dissolution of gibbsite and TCA precluded calculation of reaction kinetics for these phases.

Conclusion

Rehabilitation of alkaline, saline bauxite residue mud is a growing concern for the alumina industry. This study has identified a possible weathering trajectory for BRM, involving precipitation of boehmite, calcite, goethite, hematite, muscovite and sodalite, and dissolution of gibbsite and TCA. Porewater became less alkaline and saline during treatment. Reaction kinetics calculations based on an assumption of anatase insolubility indicated that some of the transformations observed at 235°C could proceed to a significant extent within decades, but may only reach equilibrium on a geological time scale. Ideally, treatments applied to bauxite residue deposits should aim to accelerate mineral transformations observed in this study. Encouraging mineral precipitation by applying elements such as Ca and Si in a dissolved or soluble form could be one way of achieving rapid precipitation. Given the potential costs associated with ongoing, long-term residue management, consideration should also be given to the viability of a 'secondary digest' step in the Bayer process, involving heating residue from the standard Bayer process to accelerate the transformations observed in this experiment. The effect of treatments applied prior to deposition (such as carbonation and seawater neutralization) and post-deposition (such as applied irrigation and gypsum) on the weathering trajectory predicted by high temperature treatment should also be investigated.

Acknowledgements

This research was supported by funding from Alcoa World Alumina Australia, BHP Billiton Worsley Alumina Pty Ltd, the Minerals and Energy Research Institute of Western Australia. Part of this research was undertaken on the Powder Diffraction beamline at the Australian Synchrotron, Victoria, Australia. The authors would like to thank Alan Jones and Chanelle Carter (Alcoa) for their assistance with experiments and analyses.

References

Francis RJ, O'Brien S, Fogg AM, Halasyamani PS, O'Hare D, Loiseau T, Ferey G (1999) Time-resolved *in-situ* energy and angular dispersive X-ray diffraction studies of the formation of the microporous gallophosphate ULM-5 under hydrothermal conditions. *Journal of the American Chemical Society* **121**, 1002-1015.

GBC Scientific Equipment Pty. Ltd. (2006) *Traces: X-Ray diffraction screen processing software and accessories*, *v 6.7.20*.

Murray J, Kirwan L, Loan M, Hodnett BK (2009) In-situ synchrotron diffraction study of the hydrothermal transformation of goethite to hematite in sodium aluminate solutions. *Hydrometallurgy* **95**, 239-246.

Schulze DG (1984) The influence of aluminum on iron oxides. VIII. Unit cell dimensions of Al-substituted goethites and estimation of Al from them. *Clays and Clay Minerals* **32**, 36-44.

Schwertmann U, Fitzpatrick RW, Taylor RM; Lewis DG (1979) The influence of aluminum on iron oxides. II. Preparation and properties of Al-substituted hematites. *Clays and Clay Minerals* **27**, 105 – 112.

Snars KE, Gilkes RJ (2009) Evaluation of bauxite residues (red muds) of different origins for environmental applications. *Applied Clay Science* **46**, 13-20.

Taylor S, Pearson N (2001) *Properties of Bayer process solids from Alcoa WA refineries and their component minerals*. Internal Alcoa report, Alcoa World Alumina, Kwinana Western Australia.